

C. Delire · S. Levis · G. Bonan · J.A. Foley · M. Coe  
S. Vavrus

## Comparison of the climate simulated by the CCM3 coupled to two different land-surface models

Received: 21 March 2001 / Accepted: 29 March 2002 / Published online: 22 June 2002  
© Springer-Verlag 2002

**Abstract** We present results from a coupled atmosphere–biosphere model CCM3/IBIS (the Community Climate Model coupled to the Integrated BIOSphere Simulator), which is designed to study the dynamic interactions between climate and vegetation and the global carbon cycle. We analyze the climate simulated by CCM3/IBIS with fixed vegetation conditions and we compare it to the climate simulated by the standard CCM3, which includes the LSM (land surface model) land-surface package. Important differences between the two models include simple parametrizations of lakes, wetlands and crops in CCM3/LSM not taken into account in CCM3/IBIS. CCM3/IBIS and CCM3/LSM share common biases (compared to observations) in the temperature field in boreal winter and in the precipitation field annually, making the atmospheric model the most probable cause of those biases. The models differ in the temperature field and surface energy balance in the Sahara annually and in the mid-to high latitudes from spring through fall. CCM3/IBIS simulates global annual air temperatures that are on average 1.7 °C higher than CCM3/LSM and 0.5 °C higher than the observed climatology. Differences in albedo and/or snow parametrization explain most of the Sahara and high-latitude temperature disagreement. Our sensitivity study with

CCM3/LSM shows that the presence of lakes and wetlands in CCM3/LSM can account for about half of the difference in temperature in summer over the lake and wetland regions of the mid-latitudes. A second sensitivity study shows that higher surface roughness length in CCM3/IBIS can also explain part of the difference in summer surface temperature in the mid-latitudes. Surface roughness length affects the surface temperature through a feedback mechanism linking surface wind speed, planetary boundary layer height, low level cloudiness and radiation.

---

### 1 Introduction

The land surface exchanges water, energy, momentum and also CO<sub>2</sub> with the atmosphere, therefore playing an important role in the climate system. Changes in the land surface properties, due to human activity or changing climate, affect those exchange processes and are likely to affect the climate itself. Given the potential importance of land surface processes in the climate system, efforts have been made to develop process-based biophysical models of land–atmosphere exchange processes and to couple them to general circulation models. There now exist a large number of land surface models that differ greatly in the choice of processes included and in the degree of complexity used to represent each process.

The vast majority of the land surface models coupled to general circulation models (GCMs) simulate the exchange of water, energy and momentum at the surface given a prescribed geographical distribution of the vegetation and soils. They are designed to simulate the climate at a time scale of a few years to a few decades when vegetation changes can be neglected. Some models also calculate the CO<sub>2</sub> exchange using a parametrization of the soil respiration flux (i.e. LSM, Bonan, 1995a, and SiB2, Sellers et al. 1996).

---

C. Delire (✉) · J.A. Foley · M. Coe  
Center for Sustainability and the Global Environment (SAGE),  
Gaylord Nelson Institute for Environmental Studies,  
University of Wisconsin, 1710 University Avenue,  
Madison, WI 53726, USA  
E-mail: cldelire@facstaff.wisc.edu

S. Levis · G. Bonan  
National Center for Atmospheric Research,  
PO Box 3000 Boulder, CO 80307-3000, USA

S. Vavrus  
Center for Climatic Research,  
Institute for Environmental Studies,  
University of Wisconsin, 1225 W Dayton St.,  
Madison, WI 53706-1695, USA

A small number of land surface models designed to be coupled to GCMs also represent the dynamics of the vegetation and the carbon cycling in vegetation and soils (i.e. TRIFFID, (Cox et al. 2000) and IBIS (Foley et al. 1996; Kucharik et al. 2000)). IBIS (Integrated BIOSphere Simulator) was built to simulate land surface processes, terrestrial carbon and nutrient cycling, and vegetation dynamics in a coherent and mechanistic way. IBIS has the capability to simulate short and long time scale processes, therefore providing an excellent tool that can be used inside a coupled atmosphere–ocean GCM. IBIS was first coupled to the GENESIS atmospheric GCM of Thompson and Pollard (Thompson and Pollard, 1995a, b) and used to study vegetation feedbacks in different climatic regimes (Foley et al. 1998, 2000; Levis et al. 1999a, b, 2000).

Here we coupled IBIS to the Community Climate Model CCM3 (Kiehl et al. 1998) in order to provide a tool to study climate-vegetation dynamics and the global carbon cycle, which LSM, the standard land surface model of the CCM3, does not do. Our first goal is to understand and document how the use of IBIS in the CCM3 affects the simulated climate. Therefore, we compare the climate simulated by CCM3 coupled with IBIS, to the climate simulated by CCM3 coupled with LSM. Both simulated climates are also compared to observations. We chose to operate IBIS with prescribed vegetation as a regular land surface model to ease the comparison with LSM.

Our second goal is a by-product of this comparison: by using two different land surface models coupled to the same GCM, we can investigate whether known biases of the GCM can be attributed to the land surface models or if they are inherent to the atmospheric part of the model.

Analyzing the results of coupled models is a difficult task because of the feedback mechanisms taking place. There have been three major efforts aimed at comparing and evaluating land surface models and GCMs. The PILPS (Project for Intercomparison of Land-surface Parametrization Schemes) activity has compared the simulation of roughly 20 land surface models separately from their host GCMs (off-line experiments) using identical observed or idealized atmospheric forcing and identical surface characteristics. These off-line experiments showed large discrepancies in the partitioning of available energy into latent and sensible heat and the partitioning of precipitation into evapotranspiration and runoff or drainage (Qu and Henderson-Sellers 1998). The Atmospheric Model Intercomparison Project (AMIP) (Gates 1992; Gates et al. 1999) and the Paleoclimate Modelling Intercomparison Project (PMIP) (Braconnot 2000) aimed at comparing the climate simulated by 20 to 30 different AGCMs for present and past conditions. The models were run at different resolutions with different land surface boundary conditions and different parametrizations of, among others, land surface processes. Diagnosing if the land surface is the origin of the differences among the results of the models

is a particularly difficult exercise when the atmospheric models are different. One conclusion that could be drawn from this exercise is that the land surface is not a reliable indicator of a model's ability to simulate precipitation (Boyle 1998). Here, by comparing two different land surface models in the same GCM, we can begin to see whether known biases of the GCM can be attributed to the land surface models or if they are inherent to the atmospheric part of the model.

---

## 2 IBIS-2 and LSM: model descriptions

In this study, we use an updated version of the Integrated Biosphere Simulator (IBIS) of Foley et al. (1996) and Kucharik et al. (2000). IBIS (version 2) is a comprehensive model of terrestrial biospheric processes, and includes land-surface physics, canopy physiology, plant phenology, vegetation dynamics and competition, and carbon cycling. The IBIS land surface module simulates the energy, water, carbon, and momentum balance of the soil-vegetation-atmosphere system on a short time step consistent with GCMs (~20 to 60 min). The land surface module borrows much of its basic structure from the LSX land surface package. (Thompson and Pollard 1995a, b) The module includes two vegetation layers (i.e., “trees” and “grasses and shrubs”) and six soil layers to simulate soil temperature, soil water, and soil ice content over a total depth of 4 m. Physiologically based formulations of  $C_3$  and  $C_4$  photosynthesis, (Farquhar et al. 1980) stomatal conductance (Collatz et al. 1991, 1992) and respiration (Amthor 1984) are used to simulate canopy gas exchange processes. This approach provides a mechanistic link between the exchange of energy, water, and  $CO_2$  between vegetation canopies and the atmosphere. Budburst and senescence depend on climatic factors following the empirical algorithm presented by Botta (2000). The annual carbon balance allows the vegetation dynamics sub-model to predict the maximum leaf area index and biomass for 12 plant functional types, which compete for light and water. The model can also operate with a fixed vegetation distribution, which is used in this study.

LSM (Bonan 1996) does not differ much from the land surface module of IBIS and, conceptually, fulfills the same purpose by simulating the exchange of energy, water, carbon, and momentum at the land–atmosphere interface. Vegetated surfaces include up to three plant types per grid cell distributed in patches. Lakes and wetlands (Cogley 1991) when present, form up to two additional patches per grid cell. The model operates independently within each subgrid patch, although the same atmospheric forcing applies to the entire grid cell. A set of land cover types (Olson et al. 1983), combined with corresponding plant types, and their monthly leaf areas (Dorman and Sellers 1989) describe the landscape. This model has six soil layers to a total depth of 6.3 m. As with IBIS, photosynthesis and stomatal conductance are based on Farquhar et al. (1980) and Collatz et al. (1991, 1992) respectively. Respiration follows Bonan (1995a) and Jones (1992).

The main differences between IBIS and LSM are:

1. IBIS is able to describe vegetation dynamics and carbon cycling in the soil and vegetation, whereas LSM cannot. In this study however, IBIS is used with a prescribed vegetation map so that the vegetation dynamics and carbon cycling in soils modules are not turned on.
2. LSM includes a parametrization of inland water bodies (lakes and wetlands) (Bonan 1995b) but IBIS does not.
3. LSM includes a simple representation of crops while IBIS represents only natural vegetation types.
4. Budburst and senescence in IBIS depend on the climate. In the current version of LSM, the phenology depends solely on the calendar date.
5. Each grid cell in IBIS has a vegetation cover made up of a combination of up to 12 plant functional types. When IBIS is used with fixed vegetation, as in this study, this combination is

fixed in each grid cell and acts as a single homogeneous vegetation type. In LSM, each grid cell contains up to three patches (or tiles), each with a different single vegetation type, plus up to two more patches with lake or wetland.

6. IBIS describes two canopies, one for grasses and shrubs, and the other for trees. LSM describes one canopy, either trees or grass.
7. With IBIS, physical parameters describing the vegetation, such as canopy height or roughness length, depend on the evolution of LAI and the carbon balance. In LSM they are fixed and depend solely on the vegetation type.

### 3 Simulations and data set used

We performed a total of four 20-year simulations with the NCAR CCM3 at a resolution of T31 ( $\sim 3.75^\circ \times 3.75^\circ$ ): two main simulations and two sensitivity studies. We used LSM as the land-surface model for the first main control simulation and IBIS replacing LSM for the second. We then performed two sensitivity studies with CCM3/LSM. Fixed climatological sea surface temperatures (SSTs) were used for all the runs. We chose the T31 resolution because it is the resolution that will most likely be used in global carbon cycle studies due to computing time constraints. The last 15 years of each run are used for averaging.

Soil texture is prescribed in IBIS from the IGBP-DIS global gridded texture database (International Geosphere–Biosphere Programme – Data and Information System), (IGBP-DIS 1999) while LSM retrieves information for the soil from Webb and Rosenzweig (1993). Because the version of IBIS we used does not simulate crops and pastures, we prescribed a potential vegetation distribution (Ramankutty and Foley 1999). The ‘potential’ vegetation map is intended to represent the vegetation that would exist in a location without human intervention. LSM uses a vegetation map including crops (Fig. 1). Obvious vegetation differences between the vegetation maps used in IBIS and LSM include temperate deciduous and evergreen forests in eastern and central US and in the wheat belt of the former USSR with IBIS instead of crops with LSM. The vegetation map used in IBIS has tropical deciduous forest in India and temperate deciduous forests in northeast China, where crops are imposed in LSM. In IBIS’s vegetation map, the northern treeline in North America and Russia is one grid cell further north and the vegetation cover is denser NE of Lake Baikal. With the exception of crops and the location of the northern treeline, the distribution of the major vegetation types is similar between the two models.

The distribution of lakes and wetlands in CCM3/LSM is derived from a map produced by Cogley (1991). Concentrations of inland water bodies are found in NW Canada, in the Great Lakes region, in Quebec, at the mouth of the Parana river and in the Pantanal in South America, in Finland and NW Russia, in the lakes region of east Africa, and in the Siberian lowlands (Fig. 1).

The two models were built for different purposes, describe different processes and will continue to be used with their fundamental differences. Therefore, we chose to compare them with the datasets they are usually run with. This comparison is needed to illustrate the differences that can be expected from running those two versions of CCM3. Running the models with their original datasets makes the comparison of the models more difficult: unequal results can be due to differences in the boundary conditions and/or in the parametrizations of the processes. We performed sensitivity studies to isolate factors responsible for the differences in the simulated climate.

### 4 Differences in simulated climate

#### 4.1 Temperature

CCM3/IBIS and CCM3/LSM differ greatly in the simulation of the near-surface temperature. Compared to the observed average temperatures for 1961–1990 from the Climate Research Unit of the University of East Anglia, Norwich (New et al. 1999, hereinafter referred to as CRU05), IBIS’s reference height temperatures are overestimated in most parts of the world while LSM’s are underestimated (Table 1). On a global average, IBIS is  $0.5^\circ\text{C}$  higher than the CRU05 climatology while LSM is  $1.5^\circ\text{C}$  lower. Reference height temperatures on the continents simulated by CCM3/IBIS are on the average  $2.1^\circ\text{C}$  higher than for CCM3/LSM (Table 1). At the lowest atmospheric level (between the surface and about 65 m), the difference is on average  $1.7^\circ\text{C}$ . Air temperature is higher everywhere except in the Amazon basin, around  $10^\circ\text{N}$  in Africa, in India, and on the Tibetan Plateau (Fig. 2).

**Fig. 1.** Geographical distribution of crops, lakes and wetlands in CCM3/LSM (also major differences in land surface types between CCM3/LSM and CCM3/IBIS)

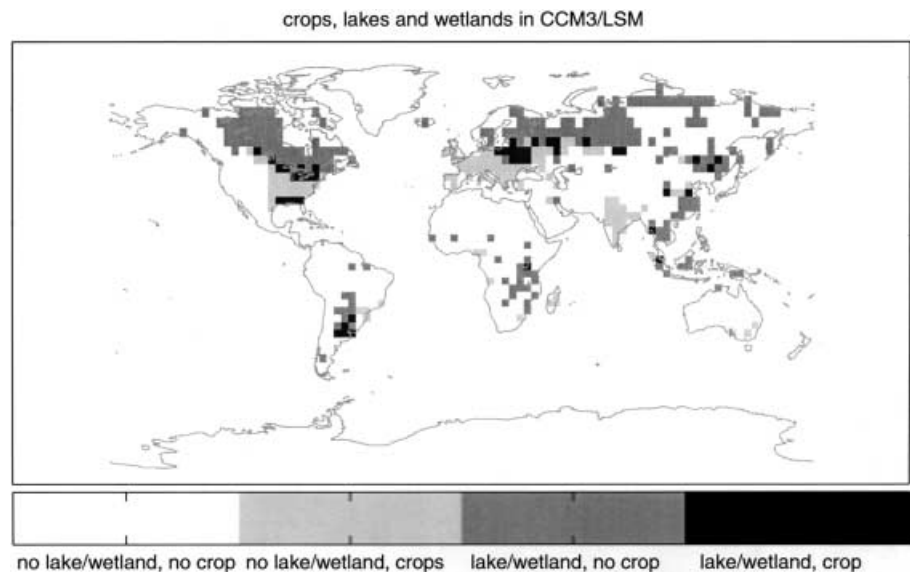


**Table 1.** Continental averages of annual reference height temperatures ( $^{\circ}\text{C}$ ) from the CRU05 climatology, (New et al. 1999), and differences between CCM3/IBIS and CRU05, and CCM3/LSM and CRU05

	CRU05	CCM3/IBIS- CRU05	CCM3/LSM- CRU05
Continents (except Antarctica)	12.6	0.5	-1.6
North America	3.7	0.8	-0.6
Europe	6.8	0.7	-0.8
Asia	4.1	0.7	-1
South America	21.8	0	-0.9
Sub-Saharan Africa	23.7	-0.6	-1.3
Oceania	22.4	0.2	-1.1
Sahara-Arabia	23.6	0.1	-2.8
Arctic	-16.0	3.5	2.3
Antarctica	/	/	/

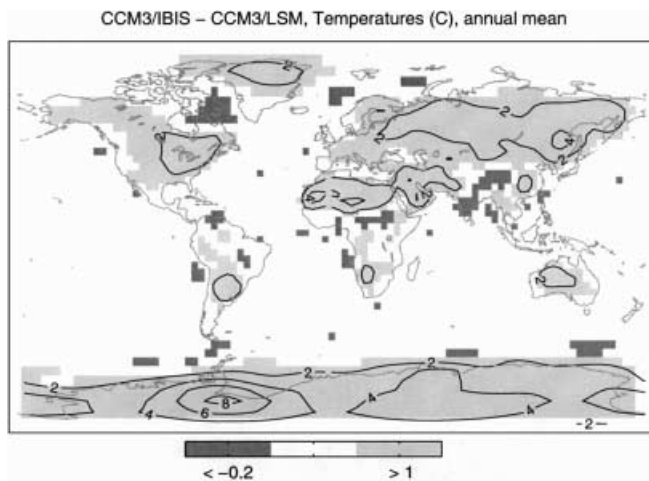


**Fig. 2.** Difference between annual mean temperature simulated by CCM3/IBIS and CCM3/LSM at the lowest GCM level (between surface and 65 m). Regions in *light (dark) gray* have temperature differences bigger than  $1^{\circ}\text{C}$  (smaller than  $-0.2^{\circ}\text{C}$ ). The *superimposed contours* indicate regions where differences are larger. The contours are displayed every  $2^{\circ}\text{C}$  from  $0^{\circ}\text{C}$ . All the differences are statistically significant at the 99% confidence level

CCM3/IBIS and CCM3/LSM have similar biases in the boreal winter: the continents around the North Atlantic are too cold as is the south of the Asian continent from Saudi-Arabia to southeast Asia, while Alaska and a band stretching from the Black Sea to northern Siberia is too warm (Fig. 3a). This was also observed in an earlier version of the CCM3 (Bonan 1998). In the boreal winter, the radiative forcing in the mid to high northern latitudes is small and the land is partly frozen so that the differences in land-surface have a minimal impact on the climate. Therefore biases in the simulated climate of the mid to high northern latitudes are most likely due to the atmospheric model. Differences between the two models include the Sahara desert  $4^{\circ}\text{C}$  too cold with CCM3/LSM as a result of possibly exaggerated high soil albedos

(Bonan 1998), the Andes too cold with CCM3/LSM and the Tibetan Plateau too cold with CCM3/IBIS.

In the other seasons, because the radiative forcing is higher in the Northern Hemisphere (where most of the continents are) the difference between the models, and the importance of the land surface becomes more apparent. CCM3/LSM is colder than the observations over most continental areas while CCM3/IBIS is warmer. In JJA, CCM3/LSM is too cold in the Sahara desert and the Arabian Peninsula, in Canada, Europe and most of Asia (Fig. 3b). On the other hand, CCM3/IBIS simulates too high temperatures in East and central USA up to northwest Canada, and in central Asia. Parts of tropical America and Africa are also too warm in JJA and SON.

The difference in temperature between the two models is not confined to the surface but influences the whole atmosphere. On average over the continents, CCM3/IBIS simulates temperatures  $0.5^{\circ}\text{C}$  higher than CCM3/LSM from 900 hPa to 200 hPa. The Northern Hemisphere continents and Antarctica contribute the most to this warmer atmosphere. In the tropics, the atmospheric column is  $0.2^{\circ}\text{C}$  warmer in the CCM3/IBIS case. As a result, the equator to pole temperature gradient is reduced with CCM3/IBIS.

The seasonal cycle of temperature is detailed in Fig. 4 for several regions of the world. Both models represent better the seasonal cycle of the Northern Hemisphere continents than the Southern Hemisphere tropical regions. The amplitude and the phase of the seasonal variations of temperature over Asia, Europe, North America, Oceania and Sahara are fairly well represented by both models. CCM3/IBIS tends to overestimate the summer temperatures especially in North America, while CCM3/LSM tends to underestimate them, especially in Asia. In the Sahara CCM3/LSM underestimates temperature by  $4^{\circ}\text{C}$  over the whole year. The seasonal cycle of temperature is more difficult to simulate in the tropics than in the mid-to high latitudes because its amplitude is very small and the temperature changes are linked to the seasonal cycle of precipitation. Both models simulate the lowest temperatures one month early in South America. In sub-Saharan Africa, both models simulate higher temperatures in October than in March instead of the opposite and the seasonal cycle with CCM3/IBIS is one month out of phase. In South America and sub-Saharan Africa, CCM3/LSM is consistently too cold while CCM3/IBIS is too warm from June to February. Both models overestimate temperatures in the Arctic regions. CCM3/IBIS is warmer than CCM3/LSM during summer in Antarctica (not covered in the CRU05 dataset).

#### 4.2 Radiation balance and cloudiness

In mid- to high latitudes, with the exception of the Tibetan Plateau, and in the Sahara desert, CCM3/IBIS simulates net shortwave radiation that is  $10\text{--}20\text{ W m}^{-2}$  higher than CCM3/LSM (Fig. 5a). This is a combined

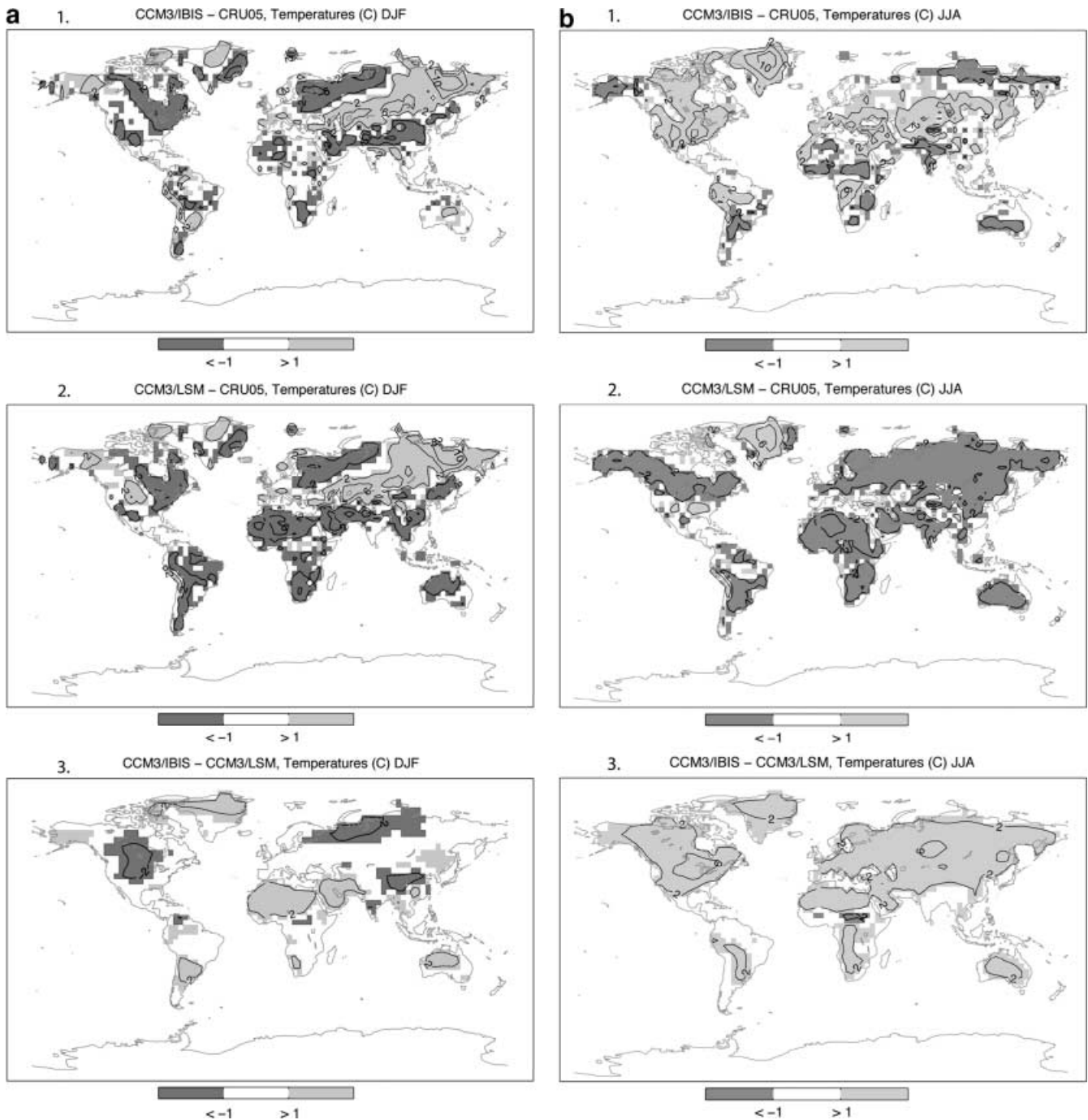


**Fig. 3.** a Air temperature differences for December, January, and February. 1 Difference between CCM3/IBIS and CRU05 climatology. 2 Difference between CCM3/LSM and CRU05 climatology. 3 Difference between CCM3/IBIS and CCM3/LSM. The temperatures used in the comparison with the CRU05 dataset are reference height temperatures. In the comparison between the two

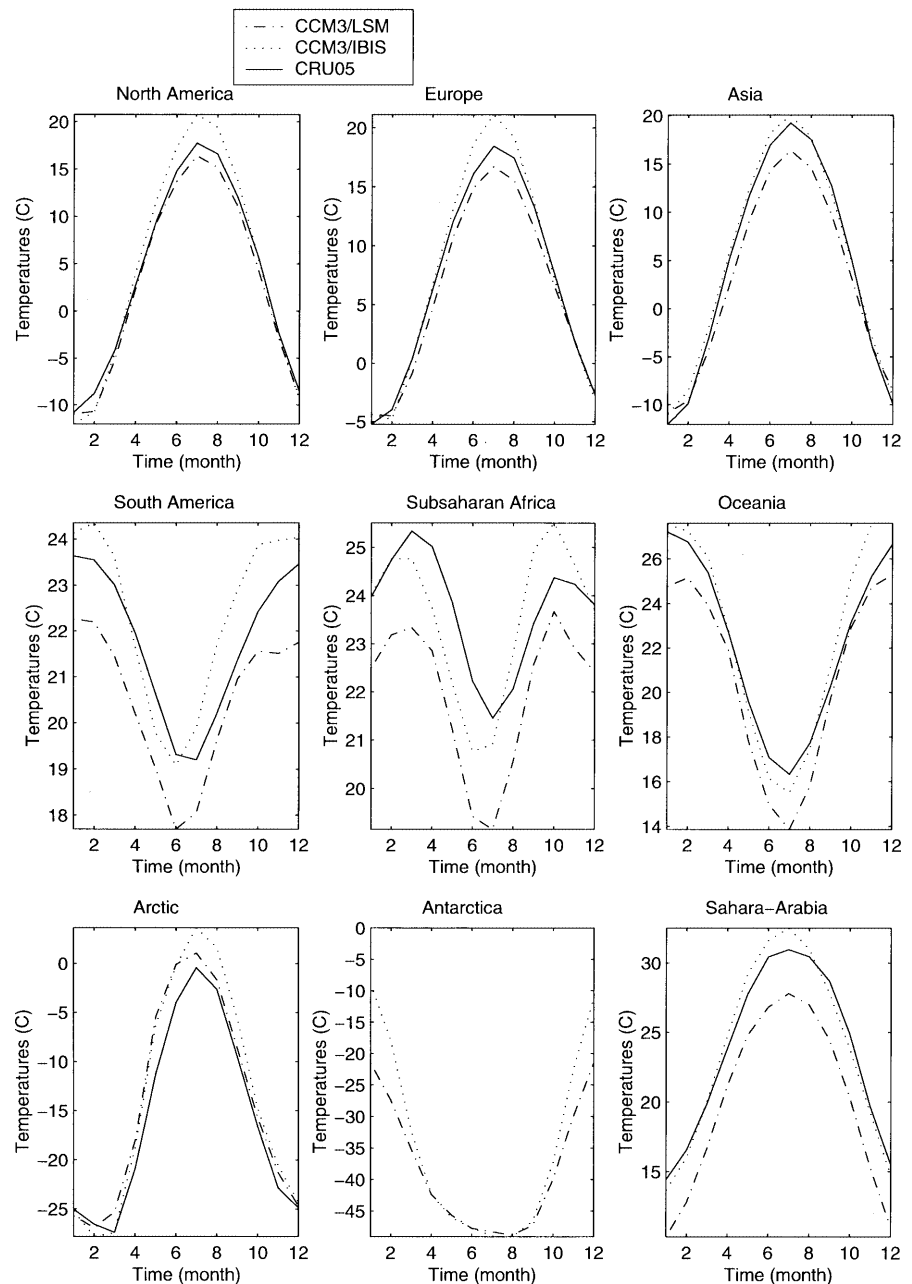
models we use the temperature at the lowest GCM level because of a different definition of reference height between the two models. *Shades of gray* have temperature differences bigger than 1 °C. Contours displayed every 4 °C from 6 °C. b Same as a but for June, July, and August

result of lower surface albedos in spring and higher incoming shortwave radiation at the surface in spring, summer and fall. The tropics receive slightly lower solar radiation because of the higher surface albedo simulated by CCM3/IBIS (Fig. 5b).

Siberia, northern Greenland, a band around Hudson Bay, southern Alaska and most of Antarctica have annual

albedos that are up to 10 to 20% lower in CCM3/IBIS (Fig. 5b). As mentioned before, albedo is also lower in the Sahara desert and in Saudi Arabia. On the other hand, CCM3/IBIS simulates slightly higher albedos on the Tibetan plateau, in the eastern and central USA, and in most of sub-Saharan Africa. The difference in albedo over the high latitude regions as well as on the Tibetan Plateau

**Fig. 4.** Evolution of monthly reference height temperatures for several regions of the world. The *black line* represents the CRU05 climatology, the *dotted line*, CCM3/IBIS and the *dash-dot line*, CCM3/LSM



is mainly due to the different snow parametrizations used in the two models. CCM3/IBIS tends to simulate a less extensive snow cover in winter and spring and a shorter snow season in Siberia, and northern Canada. CCM3/IBIS also simulates a more extensive snow cover on the Tibetan Plateau. The combination of the different snow covers and the different parametrization of the snow albedo explain the differences in albedo in most of the high-latitude regions and Tibetan Plateau.

In western Europe, Canada, eastern China and Argentina, the higher net shortwave radiation is related to higher incoming solar radiation with CCM3/IBIS, resulting from fewer low-level clouds over those regions from March through October (Fig. 5c). With CCM3/IBIS, cloudiness is reduced in the regions where surface

temperature is increased from March to October. The fact that cloudiness is lower where near-surface temperature is higher in northern summer at mid to high latitudes is in agreement with the observations (Groisman et al. 2000). The exact cause of the reduced cloudiness is hard to identify. The reduced cloudiness is consistent with reduced storm track strength. From 30°N to 55°N, westerlies are 15% weaker in CCM3/IBIS at 200 hPa in Northern Hemisphere summer. The reduced storm track activity is consistent with the reduced equator to pole temperature gradient in CCM3/IBIS.

In the tropics, the incoming shortwave radiation is lower with CCM3/IBIS and is linked to increased cloudiness (0.03 to 0.1 depending on the region) that is due to increased convective activity.

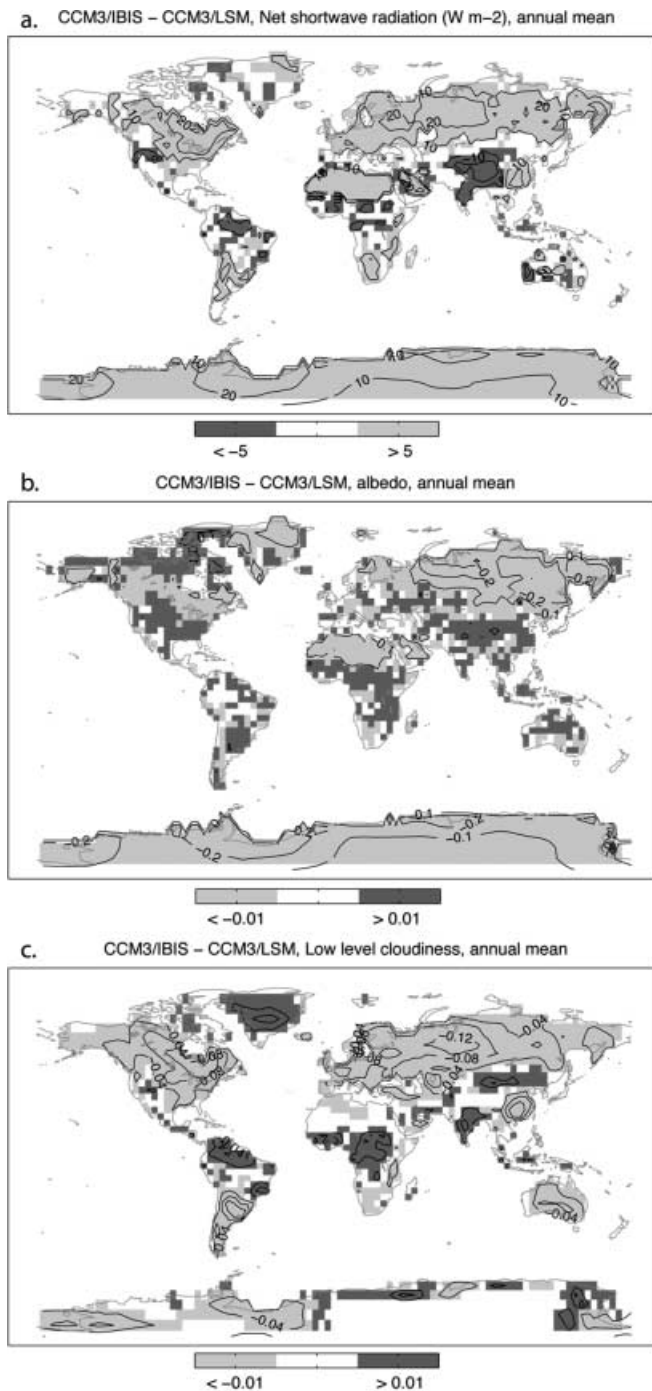


**Fig. 5a–c.** Difference between variables simulated by CCM3/IBIS and CCM3/LSM. **a** Annual mean net shortwave radiation (contour interval of  $10 W m^{-2}$ ), **b** annual mean surface albedo calculated using the mean reflected radiation and the mean incoming radiation (contour interval of  $0.01$ ), **c** annual mean low-level cloudiness (contour interval of  $0.04$ )

The combination of lower surface albedo in high latitudes and less cloudiness in mid-latitudes results in higher net solar radiation that is not compensated by longwave loss. Net radiation is therefore higher and is consistent with the higher surface temperatures. In the tropics, slightly lower net radiation is consistent with the

**Table 2.** Continental averages of annual precipitation (mm/day) from the CRU05 climatology, and differences between CCM3/IBIS and CRU05, and CCM3/LSM and CRU05

	CRU05	CCM3/IBIS- CRU05	CCM3/LSM- CRU05
Continents (except Antarctica)	2.08	0.51	0.39
North America	1.77	0.35	0.31
Europe	1.81	0.24	0.32
Asia	1.59	0.68	0.58
South America	4.19	0.28	0.07
Sub-Saharan Africa	2.77	1.04	0.82
Oceania	2.77	0.05	0.1
Sahara–Arabia	0.31	0.52	0.22
Arctic	1.32	–0.08	–0.18
Antarctica			

small negative temperature difference between the two models.

### 4.3 Precipitation

The differences between the precipitation fields simulated by the two models are much smaller than the difference between each model and the observed climatological value (Table 2). The precipitation field simulated by the CCM3/LSM presents some known biases over land (Hack et al. 1998; Bonan 1998) only slightly altered by the use of IBIS (Fig. 6), making the atmospheric model the most probable cause of those biases. In both models, precipitation tends to be locked over the major mountain ranges, the Rockies, the Andes the Tibetan Plateau and the Himalayas. The West African monsoon is displaced towards the east and there is an anomalous precipitation maximum in summer extending from the Arabian Peninsula to NE India. The southeast Asian monsoon is fairly well simulated except for an anomalous dry zone over Indochina and a maximum over the Himalayas and the Tibetan Plateau. At T31, the model overestimates total continental precipitation (Table 2).

Differences between the two models include slightly more precipitation on average with CCM3/IBIS than CCM3/LSM (Table 2). CCM3/IBIS tends to overestimate rainfall further north into the Arabian Peninsula than CCM3/LSM. This is probably due to the lower albedo over the region with IBIS. There have been numerous studies showing the importance of albedo feedback on monsoon type rainfall (see i.e., Texier et al. 2000; Brostrom et al. 1998) based on early work from Charney (1975). CCM3/IBIS does not overestimate the maximum of rainfall in northern Australia in DJF as CCM3/LSM does.

The difference in precipitation between IBIS and LSM in the tropics is due to convective precipitation, which suggests that it is a result of local differences in the land-surface parametrization. On the Northern Hemisphere continents, convective precipitation

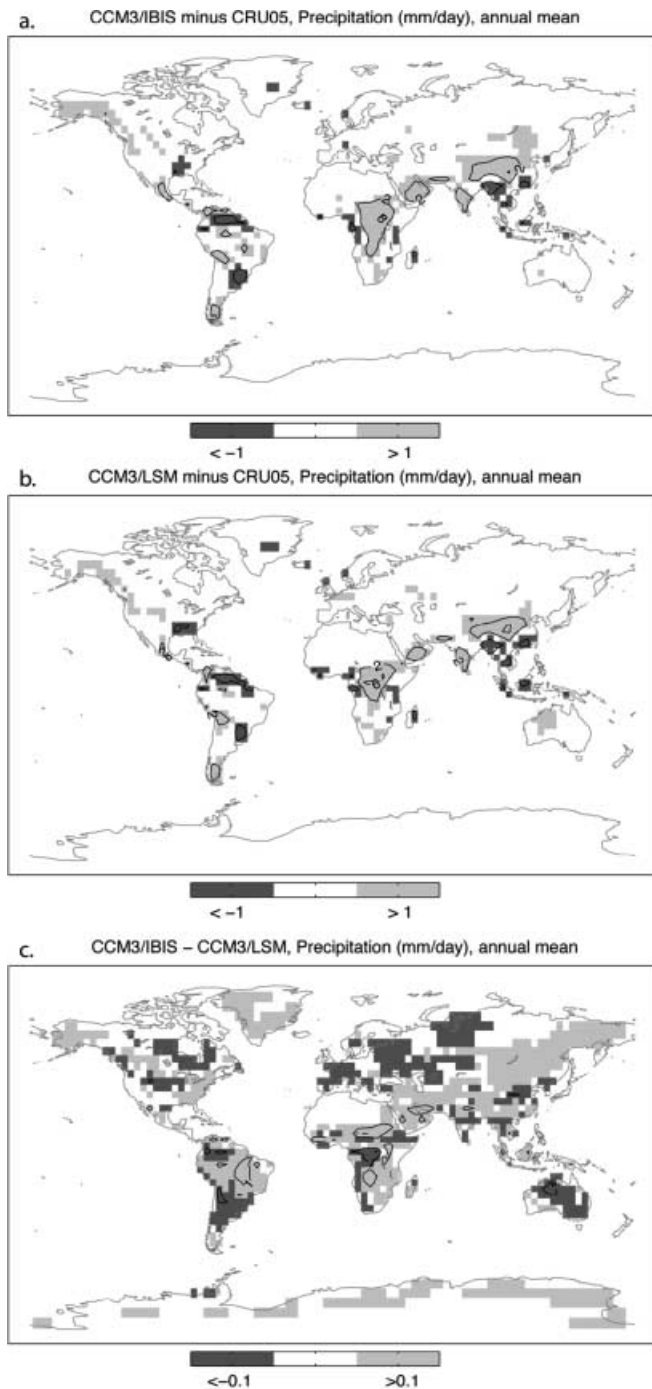


**Fig. 6a–c.** Annual mean precipitation. **a** Difference between CCM3/LSM and CRU05 climatology (contour interval of 4 mm/day, starting at  $-2$  mm/day), **b** difference between CCM3/IBIS and CRU05 climatology (contour interval of 4 mm/day, starting at  $-2$  mm/day), **c** difference between CCM3/IBIS and CCM3/LSM (contour interval of 2 mm/day, starting at  $-1$  mm/day)

accounts for less than half of the precipitation differences making large-scale atmospheric circulation the main cause for the precipitation differences.

As expected, the quality of the simulation of the precipitation field seems to be more dependent on the atmospheric model than on the land-surface represen-

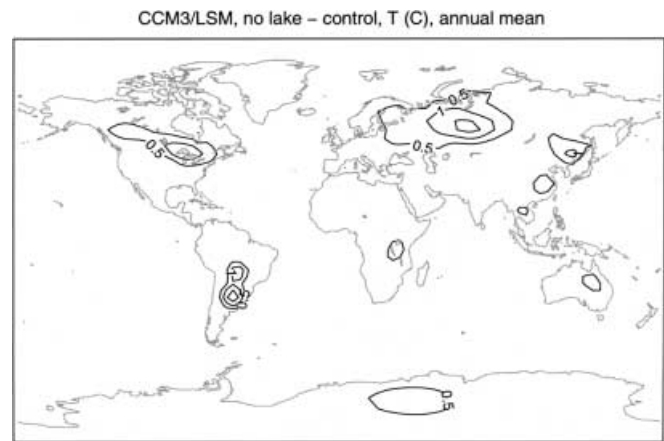


**Fig. 7.** Difference between annual mean temperature at the lowest GCM level simulated by CCM3/LSM without lakes and wetland and CCM3/LSM with lakes (control). The contour interval is  $0.5$  °C

tation despite the strong effect of the land surface on temperature over the whole atmospheric column. Using the results of AMIP experiments, Boyle (1998) showed that the land surface is not a reliable indicator of a model's ability to simulate precipitation over the USA. We reach the same conclusion with these two models on the global scale.

## 5 Effect of lakes, wetlands and crops

The fact that CCM3/LSM includes inland water bodies and crops can explain some of the differences in temperature observed between the two models. In a study with LSM coupled to CCM2, Bonan (1995b) showed that inland lakes, marshes and swamps strongly affect the surface temperature and the surface energy balance especially in the lake region of northwest Canada, the Great Lakes region of North America, the swamps in the Siberian lowlands and the lake region of east Africa. In those simulations, July surface temperatures cool by  $2\text{--}3$  °C compared to a simulation with no inland water. IBIS is  $2.5\text{--}5$  °C warmer than observed in the North American Great Lakes region in summer. This feature can at least partially be attributed to the lack of lakes and wetlands.

We ran CCM3/LSM without lakes and wetlands to evaluate their importance on the climate simulated by the CCM3. The annual mean temperatures simulated by CCM3/LSM without lakes and wetlands increase by  $0.5$  to  $2$  °C in the regions where we 'removed' the water bodies (Fig. 7). Net shortwave radiation increases by  $5$  to  $10$   $\text{W m}^{-2}$  and low-level cloudiness decreases by  $0.02$  to  $0.06$  (not shown). In the same regions, CCM3/IBIS simulates temperatures that are  $2$  to  $4$  °C higher than CCM3/LSM (with lakes),  $20$  to  $30$   $\text{W m}^{-2}$  higher net shortwave radiation and a  $0.06$  to  $0.12$  decrease in low level cloudiness. Lakes and wetlands have thus a strong

influence on the simulated climate but can only explain half the differences in temperature, radiation and cloudiness between CCM3/IBIS and CCM3/LSM over the lake and wetland regions. The lake and wetland signal is also limited to the lakes and wetland region and cannot fully account for the continental scale difference in temperature between the two models.

The second major difference in the boundary conditions between the two models consists of crops. Bonan (1999) recently showed in a simulation with CCM3/LSM that mean annual surface air temperature decreased by 0.6–1.0 °C in the United States east of 100°W after clearing of forest for agricultural land. The strongest cooling occurred in the Midwest in summer and fall. CCM3/IBIS prescribes forest and prairie in that region, which makes it likely to overestimate local temperatures compared to CCM3/LSM and to the 1961–1990 climatology. As mentioned before, cloudiness is reduced with CCM3/IBIS in the eastern USA and in Western Europe where CCM3/LSM simulates crops. As a comparison, we checked the energy balance terms and the temperature of the regions where CCM3/LSM simulates crops but has no lakes (Table 3). The air is warmer and drier over those regions with CCM3/IBIS and the planetary boundary layer is about 100 m thicker. This behavior is consistent with the cooling after deforestation obtained by Bonan (1999) for the USA. Warmer and drier air with CCM3/IBIS is not limited to the crops in the eastern USA but covers also regions with crops in Europe and Russia.

We are faced with the surprising result that CCM3/IBIS is closer to the observed temperature, even though this model ignores lakes wetlands and crops. It is likely that the effect of the lakes is overestimated or that the feedback between evaporation over the lakes and cloudiness is exaggerated so that CCM3/LSM although being more realistic than IBIS in terms of lakes and wetlands over these regions gives a wrong surface temperature. One reason for this excessive effect of the lakes might be their average depth of 50 m affecting their times of freezing and thawing as well as their temperature. The effect of the lake depth was studied with LSM in an off-line mode using atmospheric forcing. It was

shown that in this case, 50 m was an acceptable compromise. Feedbacks with the atmosphere might invalidate this conclusion.

## 6 Differences in model parametrization: roughness length

The presence of lakes, wetlands and crops in CCM3/LSM cannot explain all the differences between the climates simulated by the two models. Differences in the parametrization of the processes themselves and values of the parameters also play an important role. For example, as mentioned before, the differences in snow parametrizations result in different snow albedo, cover, and temperature. The higher prescribed albedo of the Sahara with CCM3/LSM results in surface temperatures that are 2 to 4 °C lower in that region.

IBIS and LSM also have different parametrizations of the roughness length. The roughness length impacts the planetary boundary layer (PBL) thickness simulated by CCM3 by affecting the vertical mechanical mixing and the surface energy fluxes. A rougher surface favors vertical mixing thereby increasing the PBL height. It also increases the efficiency of the sensible and latent heat fluxes, which in turn affect the PBL height. On the other hand, a rougher surface slows down the surface wind, which tends to limit sensible and latent heat.

In LSM, each vegetation type is assigned a constant roughness length. In IBIS, the overall roughness of the grid cell depends on the height of both canopies (fixed in this study) and the density of the vegetation, which depends on both the leaf and stem area indices and the fractional cover, as in LSX (Pollard and Thompson 1993). Roughness length varies thus with leaf area index following the seasonal cycle.

The mean annual roughness length in CCM3/IBIS is about 0.5 to 1.5 m greater than CCM3/LSM in southern Alaska, Canada, eastern USA, Europe, and a 10–15 °C latitude band stretching across Asia around 60°N (Fig. 8a). India, southern Congo, and the south of Brazil have roughness lengths that are 1.5 to 2 m greater with CCM3/IBIS than CCM3/LSM. The tropical forests of Brazil, central Africa and Indonesia have a slightly smaller roughness length with CCM3/IBIS. In the mid-latitudes, the largest discrepancies are located in North America, Europe, and central Asia where the large disagreement in temperature and low-level cloudiness occurs in summer (Figs. 2, 5c). The correlation coefficient between the difference in roughness length and the difference in low-level cloudiness simulated by the two models reaches –0.55 in summer on the continents north of 27°N.

There is therefore a link between roughness length at the surface, the low level clouds, and the temperature simulated by CCM3, in the mid-latitudes in spring and summer. A rougher surface increases mechanical mixing and deepens the planetary boundary layer (PBL). This effect is parametrized in CCM3 through Vogelzang and Holtzlag's (1996) formulation of PBL height in the

**Table 3.** JJA and annual averages of net radiation ( $R_n$ ), sensible heat flux ( $H$ ), latent heat flux ( $LE$ ), Bowen ratio, and reference height temperature, relative humidity ( $RH$ ) and planetary boundary layer height ( $PBLH$ ) over all the gridcells with crops (and no lakes) in CCM3/LSM

	JJA		Annual	
	CCM3/IBIS	CCM3/LSM	CCM3/IBIS	CCM3/LSM
$R_n$ ( $W\ m^{-2}$ )	128.3	127.9	86.8	87.7
$H$ ( $W\ m^{-2}$ )	44.2	39.6	27.4	29.3
$LE$ ( $W\ m^{-2}$ )	79.2	79.3	59.7	57.5
$H/LE$	0.59	0.56	0.46	0.51
$T$ (°C)	22.5	20.1	14.8	13.7
$RH$ (%)	40	68	65	69
$PBLH$ (m)	768	619	675	567

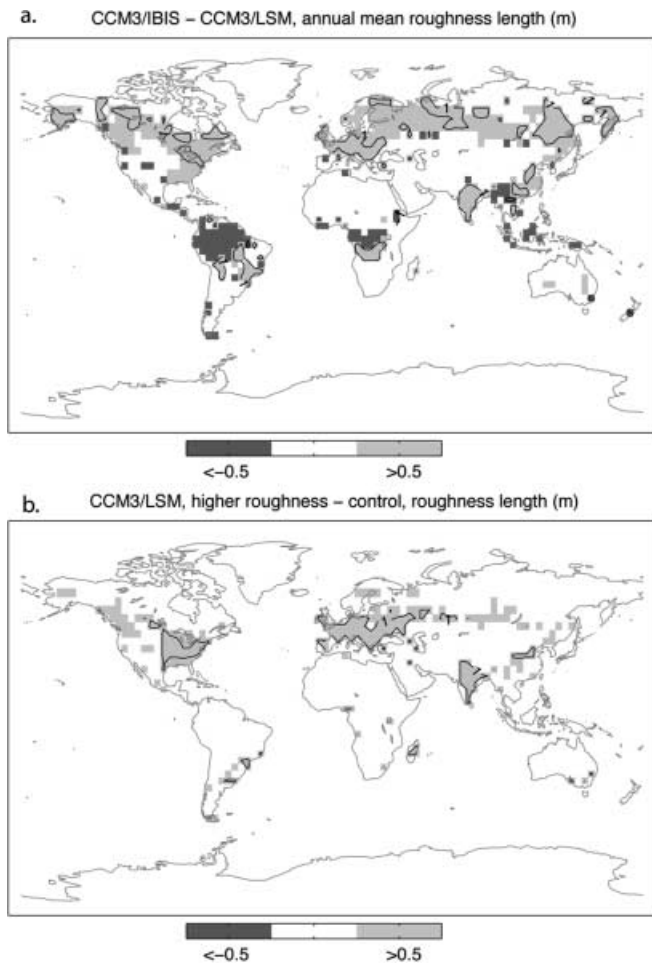


**Fig. 8a, b.** Annual mean surface roughness length (m). **a** Difference between CCM3/IBIS and CCM3/LSM, **b** difference between test and control values with CCM3/LSM. The test imposes higher roughness for crops and temperate and boreal forests. The average grid cell roughness length in CCM3/LSM is estimated as the average of the individual roughness lengths for the individual patches of vegetation. *Shades of gray* have roughness differences bigger than 0.5 m. Contour interval is 1 m

model. Since clouds are not allowed to form within the PBL, the increase in PBL height induced by the roughness length increase will decrease the cloudiness of the lower atmosphere and can result in increased surface temperature due to alterations of the surface energy balance.

We tested the sensitivity of the CCM3 climate to the roughness length with CCM3/LSM. We imposed a 1.5 m increase in roughness length for the crops and a 0.7 m increase for the temperate and boreal forests to emulate the annual mean values calculated by CCM3/IBIS. Roughness length is increased mainly in eastern USA, Europe and India (Fig. 8b). As a result of the increased roughness length, the simulated annual mean low-level cloudiness is reduced by 0.01 to 0.02 over the eastern USA, India and Europe. The annual mean temperature of the lowest atmospheric level increases by 0.5 to 1.5 °C in eastern USA, around the Mediterranean Sea and in India (Fig. 9) in CCM3/LSM. The biggest

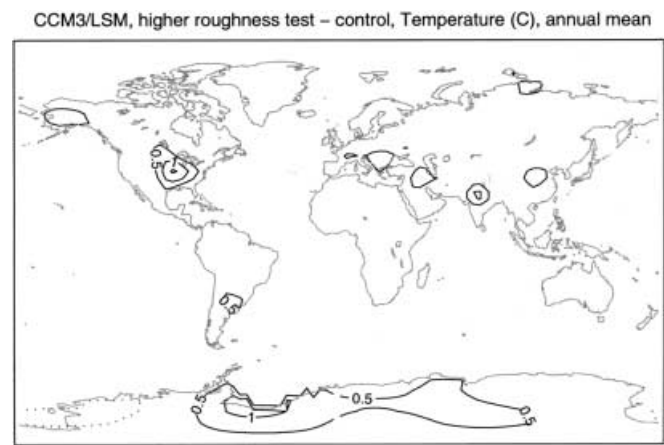


**Fig. 9.** Difference between annual mean temperature at the lowest GCM level simulated by CCM3/LSM with higher roughness (test) and the standard CCM3/LSM (control). The contour interval is 0.5 °C

increase in temperature occurs in JJA and SON and is compensated by a decrease in DJF. The increased roughness length can account for about a third of the low-level cloudiness and temperature difference between CCM3/IBIS and CCM3/LSM.

Averaged over the regions where the imposed roughness difference between the two CCM3/LSM simulations is greater than 0.5 m, surface winds decreases by  $0.42 \text{ m s}^{-1}$  in JJA, the PBL height increases by 87 m and the low level cloudiness decreases by 0.028 (Table 4). Net shortwave radiation increases (the albedo being unchanged in this sensitivity study) because of the reduced low-level cloudiness. The reduced wind speed prevents efficient sensible and latent heat transfer from the surface to the atmosphere. As a result, infrared cooling has to compensate for the increased net shortwave radiation and surface temperature increases. The increased infrared cooling decreases net radiation, which further reduces latent and sensible heating in a way that increases the Bowen ratio. This further contributes to deepen the boundary layer. This feedback mechanism was not diagnosed by Sud et al. (1988) in the study of the influence of land surface roughness on atmospheric circulation and precipitation probably because it had a fixed soil wetness and did not allow changes in clouds to affect the radiation, which plays an important role here.

We compare in Table 5 the surface energy fluxes, wind speed cloudiness and temperature simulated by CCM3/IBIS and CCM3/LSM over the regions where the roughness difference between the two models is greater than 0.5 m. The average values for CCM3/LSM differ from Table 4 because the land mask where the roughness length difference is bigger than 0.5 m is different (Fig. 8). The differences between CCM3/IBIS and CCM3/LSM are larger than the differences obtained in the sensitivity test with CCM3/LSM (Table 4) alone. For example, the reduction in cloudiness only reaches

**Table 4.** JJA and annual averages of cloudiness, net radiation ( $R_n$ ), net shortwave radiation, net longwave radiation ( $Net\ IR$ ), sensible heat flux ( $H$ ), latent heat flux ( $LE$ ), Bowen ratio, reference height temperature, surface winds and planetary boundary layer height

averaged over all the grid cells where the roughness length differ by more than 0.5 m between CCM3/LSM with higher roughness and the control case

Higher roughness	JJA		Annual	
	CCM3/LSM Control	CCM3/LSM Higher roughness	CCM3/LSM Control	CCM3/LSM Higher roughness
Low-level cloudiness	0.255	0.283	0.324	0.334
$R_n$ ( $W\ m^{-2}$ )	116.31	126.74	77.22	81.58
Net shortwave down	197.37	191.72	145.18	143.36
$Net\ IR$ up ( $W\ m^{-2}$ )	81.06	64.97	67.95	61.79
$H$ ( $W\ m^{-2}$ )	40.72	42.34	25.92	27.06
$LE$ ( $W\ m^{-2}$ )	68.56	78.15	49.66	52.81
$H/LE$	0.59	0.54		
$T$ ( $^{\circ}C$ )	18.92	18.01	10.79	10.42
Surface wind ( $m\ s^{-1}$ )	2.46	2.88	2.65	2.91
$PBLH$ (m)	703	616	618	569

**Table 5.** JJA and annual averages of cloudiness, net radiation ( $R_n$ ), net shortwave radiation, net longwave radiation ( $Net\ IR$ ), sensible heat flux ( $H$ ), latent heat flux ( $LE$ ), Bowen ratio, surface

temperature, surface winds and planetary boundary layer height averaged over all the gridcells where the roughness length differ by more than 0.5 m between CCM3/IBIS and CCM3/LSM

	JJA		Annual	
	CCM3/IBIS	CCM3/LSM	CCM3/IBIS	CCM3/LSM
Low-level cloudiness	0.275	0.362	0.368	0.419
$R_n$ ( $W\ m^{-2}$ )	118.87	112.01	75.40	70.99
Net shortwave down	189.27	170.01	136.10	123.86
$Net\ IR$ up	70.40	58.00	60.70	52.86
$H$ ( $W\ m^{-2}$ )	37.14	32.06	21.98	21.38
$LE$ ( $W\ m^{-2}$ )	76.12	70.50	53.03	47.61
$H/LE$	0.49	0.45	0.42	0.45
$T$ ( $^{\circ}C$ )	18.78	15.74	8.38	6.75
Surface wind ( $m\ s^{-1}$ )	2.04	2.45	2.02	2.61
$PBLH$ (m)	745	560	658	522

the first atmospheric layer above the PBL in the sensitivity test with CCM3/LSM. CCM3/IBIS simulates less cloudiness from the top of the PBL to the mid-troposphere, when compared to CCM3/LSM. The differences between CCM3/IBIS and CCM3/LSM are larger than in the sensitivity study because IBIS differs from LSM in many other aspects than just roughness length. The region used for averaging, for instance, includes lakes and wetlands in CCM3/LSM, which results in more low-level clouds, as mentioned in Sect. 5. Different partitioning of available solar energy into infrared cooling, sensible and latent heat in the two models also plays a role in the amplitude of the signal.

CCM3 seems therefore to have a positive feedback loop in the mid-latitudes in spring and summer between roughness, cloudiness and surface temperature. The amplitude of the signal differs between CCM3/IBIS and CCM3/LSM because of the different surface types (crops and lakes) and the different partitioning between the energy balance terms. This high sensitivity of the model to the surface roughness is troublesome considering that roughness is not well known at the large spatial scale of a GCM grid cell (see e.g., Rodriguez-Camino and Auissan 1999; Giorgi 1997).

## 7 Discussion and conclusion

One of the objectives of this study was to document the climate simulated by CCM3/IBIS, a model that will be used for studies of vegetation–atmosphere interactions and studies of the global carbon cycle and to compare it to the climate simulated by CCM3/LSM. By using the same atmospheric model with two different land-surface models, we could also begin to identify whether the biases in the simulated climate were due to the atmospheric model or to the land surface schemes. We compared two 20-year simulations: one with CCM3/IBIS and the other with CCM3/LSM, the standard land-surface scheme of the CCM3, and ran two additional sensitivity studies to help understand the differences between the two simulated climates.

The two models share common biases in the precipitation field: orographic locking of precipitation over mountain ranges, displacement of the African monsoon and excessive convective activity in central America and Africa. As in Boyle (1998), we find that the biases in the precipitation field are not affected much by the parametrization of the land-surface, which indicates that

they are probably due to the atmospheric model. Both models also share common biases in the temperature field in boreal winter when the radiation input is low in the mid to high latitudes of the Northern Hemisphere and the land, lakes and wetlands are frozen, leaving the atmospheric model the most probable reason for the biases.

Because the radiative forcing is higher from spring through fall, surface temperature and energy balance depend largely on the land surface parametrization. With CCM3/IBIS, mean annual temperatures at the lowest atmospheric level are 1.7 °C higher globally than with CCM3/LSM. The disagreement is particularly large in the Sahara, Greenland and Antarctica, and in summer over the mid-latitudes of the Northern Hemisphere where CCM3/IBIS simulates drier, hotter and less cloudy conditions. Albedo and/or snow parametrization differences between the two models explain most of the Sahara and high-latitude temperature disagreement. Our sensitivity study shows that the presence of lakes and wetlands in CCM3/LSM can account for about half of the difference in temperature in summer over the lake and wetland regions of the mid-latitudes. According to Bonan (1999), the presence of crops in CCM3/LSM can also explain part of temperature difference in the mid-latitudes. Finally, we showed with a second sensitivity study that differences in roughness length between the two models explain about a third of summer surface temperature difference through a feedback mechanism linking surface wind speed, planetary boundary layer height, low-level cloudiness and radiation. This indicates that with the two models used here, the vegetation influences the climate not only through its albedo and evapotranspiration but also through its roughness.

The results of this comparison indicate several ways to improve both CCM3/IBIS and CCM3/LSM. For example, to better represent present-day climate, we need to include a representation of crops, lakes and wetlands in CCM3/IBIS. We also need to further analyze the validity of the roughness length parametrization in the model. In CCM3/LSM, we need to correct the prescribed albedo of the Sahara and investigate the causes of the continental scale cold bias in Eurasia in summer. We also need to refine the parametrization of lakes and wetlands and further investigate the importance of lake depths on the local climate.

**Acknowledgements** We thank Marcos Heil Costa, David Pollard, Peter Snyder and Starley Thompson for valuable discussion and comments on the manuscript. This work was supported by the National Science Foundation's "Methods and Models for Integrated Assessment" program.

## References

- Amthor JS (1984) The role of maintenance respiration in plant growth. *Plant, Cell Environ* 7: 561–569
- Bonan G (1996) A land surface model (LSM version 1.0) for ecological, hydrological, and atmospheric studies: technical description and user's guide. National Center for Atmospheric Research, Boulder, CO, USA
- Bonan GB (1995a) Land-atmosphere CO<sub>2</sub> exchange simulated by a land surface process model coupled to an atmospheric general circulation model. *J Geophys Res* 100(D2): 2817–2831
- Bonan GB (1995b) Sensitivity of a Gcm simulation to inclusion of inland water surfaces. *J Clim* 8 (11):2691–2704
- Bonan GB (1998) The land surface climatology of the NCAR Land Surface Model coupled to the NCAR Community Climate Model. *J Clim* 11(6): 1307–1326
- Bonan GB (1999) Frost followed the plow: impacts of deforestation on the climate of the United States. *Ecol Appl* 9(4): 1305–1315
- Botta A, Viovy N, Ciais P, Friedlingstein P, Monfray P (2000) A global prognostic scheme of leaf onset using satellite data. *Global Change Biol* 6(7): 709–725
- Boyle JS (1998) Evaluation of the annual cycle of precipitation over the United States in GCMs: AMIP simulations. *J Clim* 11(5): 1041–1055
- Braconnot P (2000) PMIP, Paleoclimate Modeling Intercomparison Project (PMIP): Proc 3rd PMIP workshop, Canada. WCRP-111, WMO/TD-1007
- Brostrom A, Coe M, Harrison SP, Gallimore R, Kutzbach JE, Foley J, Prentice IC, Behling P (1998) Land surface feedbacks and palaeomonsoons in northern Africa. *Geophys Res Lett* 25(19): 3615–3618
- Charney JG (1975) Dynamics of deserts and drought in the Sahel. *Q J R Meteorol Soc* 101: 193–202
- Cogley JG (1991) GGHYDRO – Global hydrological data release 2.0. Trent Climate Note 91-1, Trent University – Department of Geography, Peterborough, Ontario, Canada
- Collatz GJ, Ball JT, Grivet C, Berry JA (1991) Physiological and environmental-regulation of stomatal conductance, photosynthesis and transpiration – a model that includes a laminar boundary-layer. *Agr Forest Meteorol* 54(2–4): 107–136
- Collatz GJ, Ribas-Carbo M, Berry JA (1992) Coupled photosynthesis-stomatal conductance model for leaves of C<sub>4</sub> plants. *Aust J Plant Physiol* 19: 519–538
- Cox PM, Betts RA, Jones CD, Spall SA, Totterdell IJ (2000) Acceleration of global warming due to carbon-cycle feedbacks in a coupled climate model. *Nature* 408(6813): 750–750
- Dorman JL, Sellers PJ (1989) A global climatology of albedo roughness length and stomatal resistance for atmospheric general circulation models as represented by the simple biosphere model (SiB). *J Appl Meteorol* 28: 833–855
- Farquhar GD, von Caemmerer S, Berry JA (1980) A biochemical model of photosynthetic CO<sub>2</sub> assimilation in leaves of C<sub>3</sub> species. *Planta* 149: 78–90
- Foley JA, Levis S, Costa MH, Cramer W, Pollard D (2000) Incorporating dynamic vegetation cover within global climate models. *Ecol Appl* 10(6): 1620–1632
- Foley JA, Levis S, Prentice IC, Pollard D, Thompson SL (1998) Coupling dynamic models of climate and vegetation. *Global Change Biol* 4(5): 561–579
- Foley JA, Prentice CI, Ramankutty N, Levis S, Pollard D, Sitch S, Haxeltine A (1996) An integrated biosphere model of land surface processes, terrestrial carbon balance, and vegetation dynamics. *Global Biogeochem Cycles* 10(4): 603–628
- Gates WL (1992) The Atmospheric Model Intercomparison Project. *Bull Am Meteorol Soc* 73: 1962–1970
- Gates WL, Boyle JS, Covey C, Dease CG, Doutriaux CM, Drach RS, Fiorino M, Gleckler PJ, Hnilo JJ, Marlais SM, Phillips TJ, Potter GL, Santer BD, Sperber KR, Taylor KE, Williams DN (1999) An overview of the results of the Atmospheric Model Intercomparison Project (AMIP I). *Bull Am Meteorol Soc* 80(1): 29–55
- Giorgi F (1997) An approach for the representation of surface heterogeneity in land surface models. I. Theoretical framework. *Mon Weather Rev* 125(8): 1885–1899
- Groisman PY, Bradley RS, Sun BM (2000) The relationship of cloud cover to near-surface temperature and humidity: comparison of GCM simulations with empirical data. *J Clim* 13(11): 1858–1878

- Hack JJ, Kiehl JT, Hurrell JW (1998) The hydrologic and thermodynamic characteristics of the NCAR CCM3. *J Clim* 11(6): 1179–1206
- IGBP-DIS (1999) Global soil data task: spatial database of soil properties. International Geosphere–Biosphere Programme – Data and Information System, Toulouse, France
- Jones HG (1992) Plants and microclimate: a quantitative approach to environmental plant physiology. Cambridge University Press, Cambridge, UK, pp 428
- Kiehl JT, Hack JJ, Bonan GB, Boville BA, Williamson DL, Rasch PJ (1998) The National Center for Atmospheric Research Community Climate Model: CCM3. *J Clim* 11(6): 1131–1149
- Kucharik CJ, Foley JA, Delire C, Fisher VA, Coe MT, Lenters JD, Young-Molling C, Ramankutty N, Norman JM, Gower ST (2000) Testing the performance of a dynamic global ecosystem model: water balance, carbon balance, and vegetation structure. *Global Biogeochem Cycles* 14(3): 795–825
- Levis S, Foley JA, Pollard D (1999a) CO<sub>2</sub>, climate, and vegetation feedbacks at the Last Glacial Maximum. *J Geophys Res Atmos* 104(D24): 31,191–31,198
- Levis S, Foley JA, Pollard D (1999b) Potential high-latitude vegetation feedbacks on CO<sub>2</sub>-induced climate change. *Geophys Res Lett* 26(6): 747–750
- Levis S, Foley JA, Pollard D (2000) Large-scale vegetation feedbacks on a doubled CO<sub>2</sub> climate. *J Clim* 13(7): 1313–1325
- New M, Hulme M, Jones P (1999) Representing twentieth-century space-time climate variability. Part I: development of a 1961–90 mean monthly terrestrial climatology. *J Clim* 12(3): 829–856
- Olson JS, Watts JA, Allison LJ (1983) Carbon in live vegetation of major world ecosystems. ORNL-5862, Oak Ridge National Laboratory, Oak Ridge, Tenn, USA
- Pollard D, Thompson SL (1993) Description of a land-surface-transfer model (LSX) as part of a global climate model. National Center for Atmospheric Research, Boulder, CO, USA
- Qu WQ, Henderson-Sellers A (1998) Comparing the scatter in PILPS off-line experiments with that in AMIP I coupled experiments. *Global Planet Change* 19(1–4): 209–223
- Ramankutty N, Foley JA (1999) Estimating historical changes in global land cover: croplands from 1700 to 1992. *Global Biogeochem Cycles* 13(4): 997–1027
- Rodriguez-Camino E, Avissar R (1999) Effective parameters for surface heat fluxes in heterogeneous terrain. *Tellus Ser a-dyn Meteorol Oceanogr* 51(3): 387–399
- Sellers PJ, Randall DA, Collatz GJ, Berry JA, Field CB, Dazlich DA, Zhang C, Collelo GD, Bounoua L (1996) A revised land surface parametrization (SiB2) for atmospheric GCMs. 1. Model formulation. *J Clim* 9(4): 676–705
- Sud YC, Shukla J, Mintz Y (1988) Influence of land surface-roughness on atmospheric circulation and precipitation – a sensitivity study with a general-circulation model. *J Appl Meteorol* 27(9): 1036–1054
- Texier D, de Noblet N, Braconnot P (2000) Sensitivity of the African and Asian monsoons to mid-Holocene insolation and data-inferred surface changes. *J Clim* 13(1): 164–181
- Thompson SL, Pollard D (1995a) A global climate model (GENESIS) with a land-surface transfer scheme (lsx). Part II: CO<sub>2</sub> sensitivity. *J Clim* 8(5): 1104–1121
- Thompson SL, Pollard D (1995b) A global climate model (GENESIS) with a land-surface-transfer scheme (LSX). Part I: present-day climate. *J Climatol* 8: 732–761
- Vogelzang DHP, Holtslag AAM (1996) Evaluation and model impacts of alternative boundary-layer height formulations. *Boundary-Layer Meteorol* 81: 245–269
- Webb RS, Rosenzweig CE (1993) Specifying land surface characteristics in general circulation models: soil profile data set and derived water-holding capacities. *Global Biogeochem Cycles* 7(1): 97–108